Visualization and characterization of gastric contractions using a radionuclide technique

J.-L. C. URBAIN, E. VAN CUTSEM, J. A. SIEGEL, S. MAYEUR, A. VANDECRUYS, J. JANSSENS, M. DE ROO, AND G. VANTRAPPEN
Nuclear Medicine Department and Gastroenterology Division, University Hospital Gasthuisberg, 3000 Leuven, Belgium; and Nuclear Medicine Section, Temple University Hospital, Philadelphia, Pennsylvania 19140

URBAIN, J.-L. C., E. VAN CUTSEM, J. A. SIEGEL, S. MAYEUR, A. VANDECRUYS, J. JANSSENS, M. DE ROO, AND G. VANTRAPPEN. *Visualization and characterization of gastric contractions using a radionuclide technique.* Am. J. Physiol. 259 (Gastrointest. Liver Physiol. 22): G1062–G1067, 1990.—With the use of the radionuclide gastric-emptying test and a new data processing method, the contraction characteristics of the stomach were analyzed. After ingestion of a radiolabeled test meal, dynamic images of the stomach were acquired and analyzed to determine the frequency, amplitude, and rate of gastric contractions in healthy subjects. The frequency of antral contractions was found to be inversely related with food retention in the stomach; in contrast, the amplitude of the contractions decreased progressively during the course of gastric emptying. The peaks of both antral contraction and filling rate and the time of their occurrence remained constant throughout gastric emptying. The observed patterns of phase distribution and sequential phase changes of the food in the stomach confirmed noninvasively what was already known from invasive technique, i.e., that the proximal stomach does not undergo phasic contractions and that, in the distal stomach, smooth muscle contraction originates in midcorpus and propagates aborally to the pylorus. The scintigraphic test can be used to noninvasively and quantitatively characterize gastric motor function and to delineate the spatial sequence of gastric contractions. This technique can be applied to study the pathophysiology of gastric emptying in various motor disorders.

gastric emptying; contraction amplitude; phase image

INTRALUMINAL MANOMETRY and mucosal electrogastrography are the methods of reference to determine the electromechanical activity of the stomach in fasting subjects. After feeding, characterization of human gastric motility is difficult to achieve by internal recording because peristaltic waves are not always lumen obliterating (19) and electrodes detach from the mucosa in response to mucus secretion and excess gastric wall motion (2). Contrast radiography (5, 6) and real-time ultrasonography (12, 13) have been used to visualize postprandial antral contractions. However, these procedures have technological limitations and cannot be routinely employed to characterize the mechanical activity of the human stomach. Introduced by Griffith et al. (9) in 1966, the isotopic gastric-emptying procedure is now considered by gastroenterologists as the reference test to noninvasively evaluate gastric emptying in normals and patients. The fundamental principle of the test has not changed since its introduction and basically consists of determining the quantity of radiolabeled food remaining in the stomach over time after ingestion of a test meal. With the use of this approach, radioscintigraphy provides information only on transit of the food in the stomach and gives no insight on gastric contractions. In this study, we have developed and validated a scintigraphic method to visualize and characterize gastric contractions in normal subjects.

MATERIALS AND METHODS

Population. Ten healthy male volunteers (mean age 23 ± 2 yr) were studied. All denied consumption of drugs or alcohol and none had gastrointestinal complaints or a history of gastrointestinal surgery. The study was approved by the Ethical Committee of Gasthuisberg University Hospital on November 13, 1988, and informed consent was obtained from each volunteer.

Scintigraphic procedure. After an overnight fast, each subject received a standardized meal consisting of 20 g beaten raw egg labeled with 3 mCi ^{99m}Tc-sulfur colloid and steam cooked in a hot water glass tube, 2 slices of white bread with 5 g margarine, 60 g low-fat cream cheese, and 150 ml of water. This test meal weighed 285 g and contained 200 kcal consisting of 20% fat, 30% carbohydrate, and 50% protein. The radiation burden associated with this study was 1.38 rads for the upper large intestine (the target organ) and 0.054 rads for the whole body (18).

Immediately after ingestion of the meal, each volunteer was seated between the two heads of a dual-headed gamma camera that was equipped with parallel-hole low-energy collimators and was interfaced to a computer. Simultaneous anterior and posterior static 128 × 128

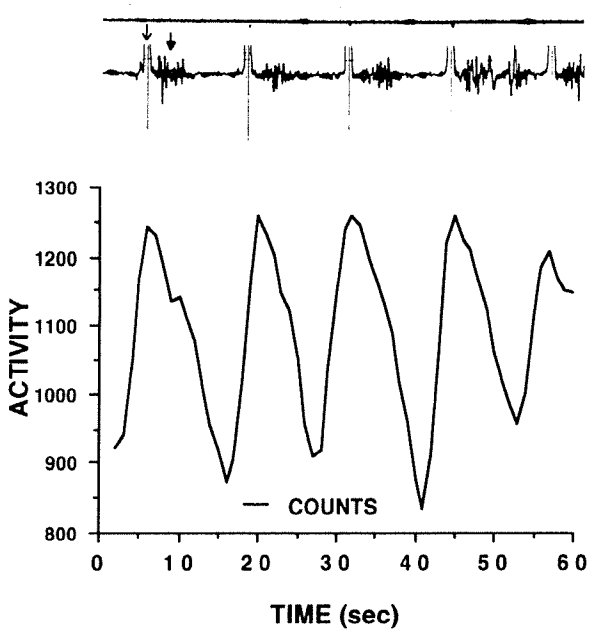

FIG. 1. Correlation between a 60-s antral activity curve (*bottom*) and corresponding electrogastrogram (*top*) recorded in a dog. Each antral activity cycle corresponds to spike potentials (closed arrow), which follow a slow-wave potential (open arrow).

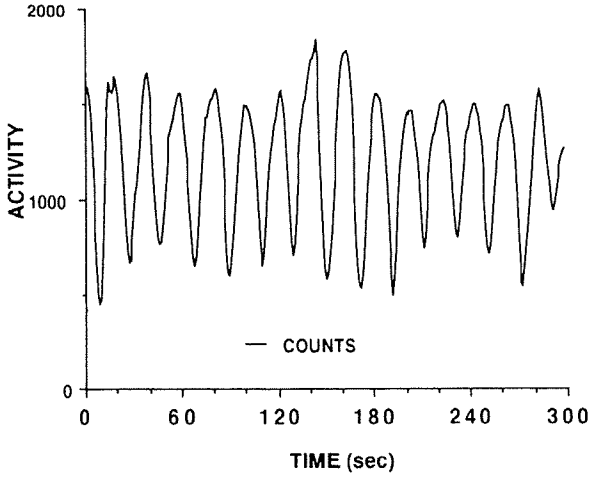

FIG. 2. An antral time-activity curve for a whole set of 5 min dynamic acquisition in one volunteer. Pattern of the curve is sinusoidal and cycles can be defined by a peak-curve finding algorithm.

pixels matrix images were acquired using the 140 keV ^{99m}Tc photopeak with 20% energy windows for 1 min every 10 min for 2 h. All images were decay corrected. Regions of interest were drawn around each image of the stomach, and for each time interval geometric mean counts were generated from the square root of the product of anterior and posterior counts. Percentage of activity remaining in the stomach was then determined.

Anterior images of the stomach were also acquired for 5 min in list mode (very fast dynamic frames of 50-ms each) using a 64 × 64 pixels matrix with a 2.6 acquisition zoom at 15, 31, 61, 91, and 121 min. After decay correction, each set of list-mode frames was compiled into a 5-min static image to clearly visualize the proximal and distal stomach and to draw a raw region of interest around the antrum. Frames of 250-ms each were then generated. An edge-detection algorithm based on the detection of the abrupt change in radioactivity between the background and the content of the stomach was applied to each frame to precisely and consistently outline the antrum. Antral time-activity curves were generated. Because the amount of radioactivity within the antrum is directly proportional to the amount of food, changes in the antral time-activity curve parallel changes in antral volume and reflect antral movements, i.e., mainly antral contractions. The sinusoidal curves obtained were fit using the first harmonic of the Fourier series to determine the frequency (CF) and the amplitude (CA) of antral contractions. A curve-peak finding algorithm was then applied to each time-activity curve to indicate the start of every gastric cycle.

List mode-images were then reframed into 20 images/cycle, and for each 5-min set of dynamic acquisition, 20 pseudogated images consisting of the sum of the same number frame interval in every cycle and a single composite time-activity curve were generated. Repeated viewing of the 20 frames of the pseudogated image in rapid sequence on the computer gave the dynamic motion of the gastric walls. The peak contraction rate (PCR), peak filling rate (PFR), time-to-peak contraction rate (TPCR), and time-to-peak filling rate (TPFR) were calculated using the first derivative of the function for each filtered composite time-activity curve. The first harmonic Fourier analysis of the time-activity curve in each gastric pixel location of the 20 pseudogated images allowed for the determination of the pixels that had the same relative timing on the composite curve. Assembling pixels with the same timing during the gastric cycle on a color scale created phase images. The closed-loop cinematic display of the phase images during a gastric cycle enables visualization of the progression of the wave of gastric contraction for that cycle.

TABLE 1. *Gastric contraction parameters*

Parameter	Time, min				
	15	30	60	90	120
CF, cycle/min	2.9±0.32	2.9±0.14	3.12±0.32*	3.21±0.18*	3.41±0.28*
CA, %	56.6±8.8	54.8±5.2*	48.2±9.6*	46.6±7*	37.8±8.9*
PCR, $\%\cdot s^{-1}$	13.9±1	13.2±2	14±2	13.5±0.5	14.1±1
TPCR, s	8.39±1.58	7.62±0.65	8.06±1.09	8.01±0.47	7.89±0.77
PFR, $\%\cdot s^{-1}$	18.2±3.4	16.7±3.1	17.9±1.3	16.9±2.2	19.0±2.5
TPFR, s	13.8±1.6	12.2±2.3	12.3±1.1	11.91±2	12±1.33

Values are means ± SD. CF, contraction frequency; CA, contraction amplitude; PCR, peak contraction rate; TPCR, time-to-peak contraction rate; PFR, peak filling rate; TPFR, time-to-peak filling rate. * $P < 0.05$ vs. 15 min.

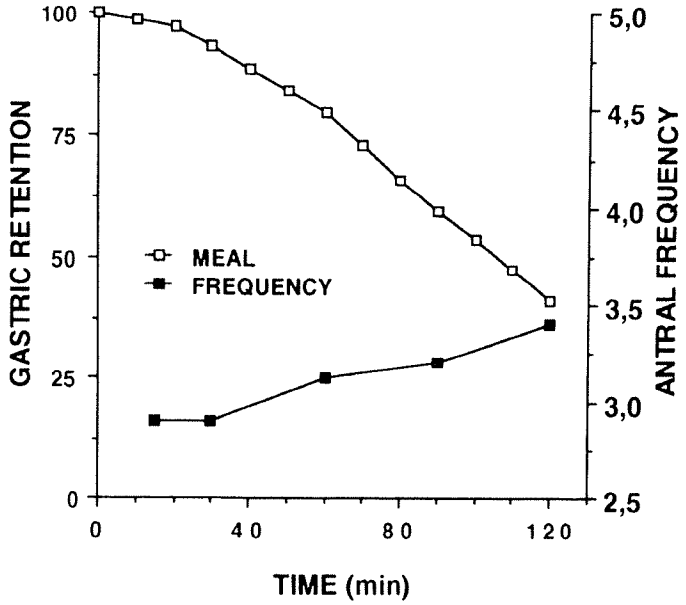

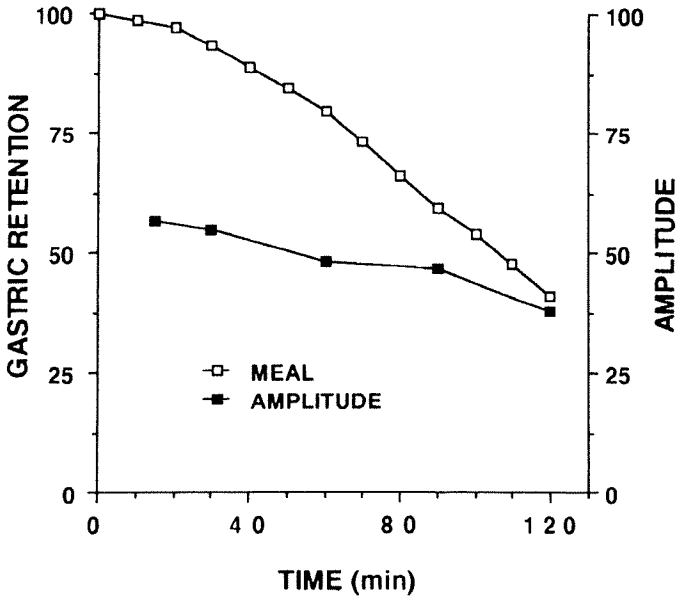

FIG. 3. Antral frequency (*top*) and amplitude (*bottom*) data are plotted with percentage of meal retention on double *y*-axis graphs. Frequency of antral contractions increases slightly as gastric emptying progresses. In contrast, amplitude of these contractions decreases significantly.

Animal validation. Correlations between the antral time-activity curve cycle and gastric contractions were established in five dogs using the serosal electrogastrographic technique. Three weeks after surgical implantation of four bipolar silver chloride electrodes distributed from the terminal antrum to the proximal fundus, each dog underwent the isotopic procedure described above. Simultaneous isotopic and serosal electrogastrographic recordings were obtained. Scintigraphic data were processed as previously described to individualize the gastric cycles, and the electrogastrographic tracings were analyzed visually to determine the electrical spike activity. The ratio of the number of isotopic cycles to the number

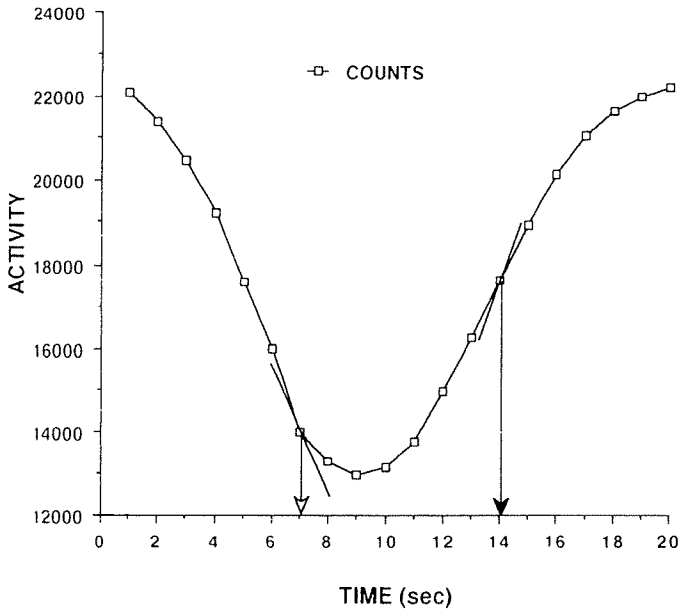

FIG. 4. Composite antral time-activity curve obtained by gating all the cycles of a dynamic acquisition set. Curve can be characterized by the maximum variation of counts/s during contraction, i.e., peak contraction rate (PCR), and during the subsequent filling period, i.e., peak filling rate (PFR). The time at which these values are maximal characterizes the time-to-peak contraction rate (TPCR) and the time-to-peak filling rate (TPFR). They are represented by slope lines (PCR, PFR) and open (TPCR) and solid (TPFR) arrows.

of plateau potentials was calculated for each list-mode acquisition period.

Statistical analysis. The contraction parameters (CF, CA, PCR, TPCR, PFR, and TPFR) were compared for each dynamic set of imaging using Student's paired *t* test. Correlations between isotopic cycles and plateau potentials were analyzed using the *r* coefficient. The goodness of the Fourier fit for the time-activity curves was evaluated using a χ^2 algorithm that calculates the sum of the squares of the differences, at each time interval, between the observed values and the values obtained by the fitting function.

RESULTS

Correlation between isotopic cycles and plateau potentials. Correlation between the time-activity curve and the simultaneous serosal electrogastrogram of the canine gastric antrum for a period of 1 min is shown in Fig. 1. Each isotopic antral cycle was clearly distinct and corresponded to an electrographic signal that was characterized by a slow wave followed by spike potentials. The ratio of the frequency of isotopic gastric cycles obtained using the first harmonic Fourier transform to the number of spike bursts was close to unity for each set of dynamic acquisitions in each dog ($r = 0.97$).

Time-activity curves. A 5-min time-activity curve obtained in a normal human is shown in Fig. 2. The curves obtained were sinusoidal in shape, and Fourier analysis resulted in excellent fits (mean χ^2 35 $\pm$ 10) for the determination of the frequency and the amplitude of the antral activity changes. Frequencies were expressed as the mean number of antral cycles per minute for each 5

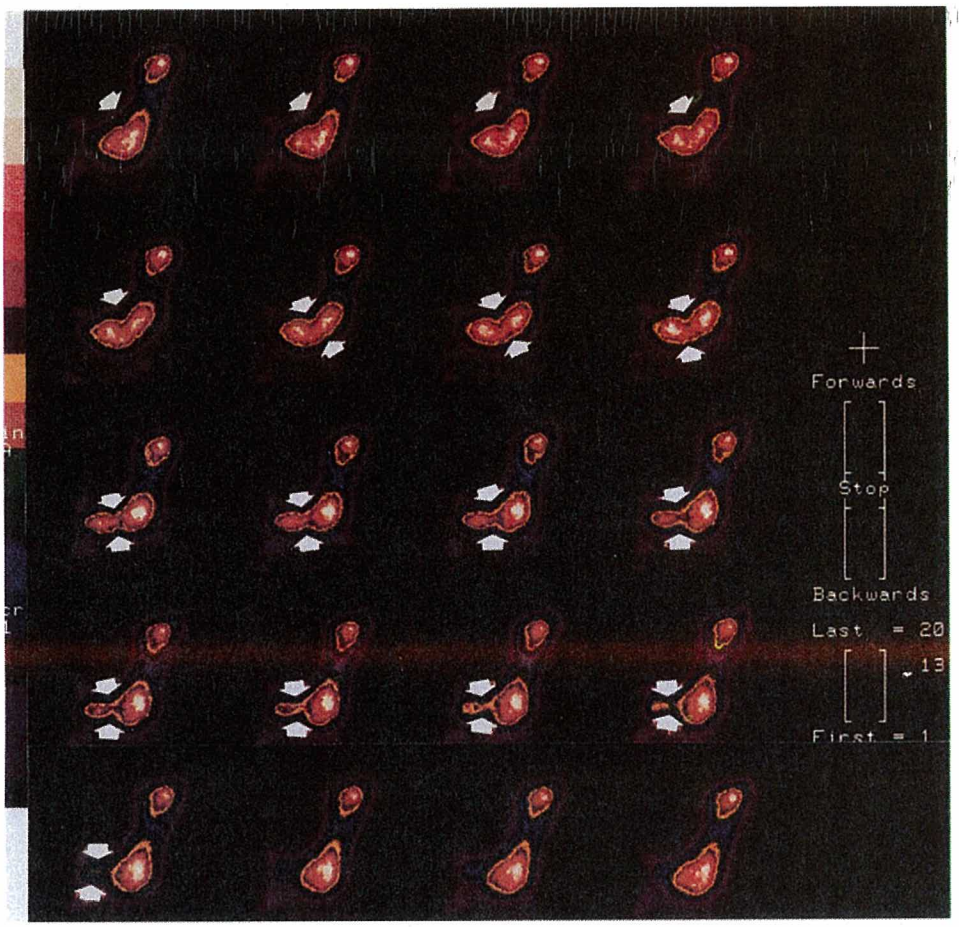

FIG. 5. Progression of gastric wall movements from the caudad corpus to the terminal antrum is shown in 20 images sequenced from top to bottom and from left to right. Initially, food is compacted in the upper portion of the distal stomach (*images 1* and *2*). The superficial indentation of the lesser curvature seen on first 2 images becomes deeper as it progresses to the antrum (*images 3–6*) and forms a contraction ring with an opposite depression on the greater curvature (*image 6*). Contraction wave progressively sweeps the antral content (*images 7–17*) forward and then retropells it back into the body of the stomach (*image 18–20*).

min of imaging; the amplitude was defined as the mean percentage of the counts variation for each 5-min acquisition set.

A slight but significant increase in frequency (Table 1 and Fig. 3, *top*) and a significant decrease in amplitude of antral contractions (Table 1 and Fig. 3, *bottom*) were observed during gastric emptying.

Gastric contraction parameters. A composite time-activity curve is shown in Fig. 4. The first and second derivative function analysis of each composite time-activity curve allowed characterization, for each dynamic set of acquisition, of the PFR and PCR in percent of counts variation per second as well as the TPFR and TPCR in seconds (Table 1). In contrast to the frequency and amplitude variation, the PCR, TPCR, PFR, and TPFR parameters showed no statistically significant variation during gastric emptying.

Gastric contraction images. The 20 images in Fig. 5 show the progression of gastric wall movements from the caudad corpus to the terminal antrum during one gastric cycle. Images are sequenced from top to bottom and from left to right. At the beginning (*images 1* and *2*) the food in the distal stomach is compact, and a slight depression of the gastric wall can be seen (white arrow) on the lesser curvature. This depression becomes more indented when progressing to the antrum (*images 3–6*) and is accompanied by a similar movement of the greater curvature wall. Both waves then progress simultaneously, generating a ring of contraction that closes the antrum (*images 8–17*) and retropells most of the antral content (*images 18–20*).

Phasic activity of the stomach. The global phase image of the stomach (Fig. 6) allowed visualization of the movement of gastric content in the different regions of the stomach on a color scale. A unique color, i.e., a unique phase, is seen in the proximal stomach, indicating that this part of the stomach does not undergo any phasic activity. In contrast, the two complete color shades observed in the more distal stomach clearly show the phase progression of a contraction in the antrum and the following one in the corpus as it is often observed in healthy subjects. The color scale clearly demonstrated that the contraction in the corpus begins in a zone located along the greater curvature at the junction of the proximal and distal stomach that is thought to function as the gastric pacemaker (19).

DISCUSSION

A century ago, Cannon (5) used Röentgen rays to describe the motor activity of the cat stomach. More recently, Carlson et al. (6) characterized the motor action of the canine gastroduodenal junction by means of cineradiography. Real-time ultrasonography has also been used to visualize antral contractions (12, 13). These techniques, however, do not allow quantitative characterization of the postprandial gastric contractions, and, so far, our understanding of postprandial gastric motor

FIG. 6. Global phase image of the stomach represents different levels of mechanical activity of the various portions of the stomach in a color scale (*left*). Proximal stomach is mainly a tonic muscle without phasic contractions; it has no phase variation and is colored black. In contrast, the distal stomach shows a complete phase progression (scaled from purple to black) that is a complete mechanical cycle in the antrum and in the corpus. The < sign indicates the origin of the contraction in the corpus.

activity is based on data derived from intraluminal manometry and electromyography in experimental animals (7, 8, 10, 11, 14, 15) and electrogastrographic recordings in human subjects (1, 20, 21).

Using the radionuclide technique, present computer capabilities, and a new approach for the analysis of the dynamic imaging of gastric emptying, we have shown in this study that it is possible to visualize changes in antral food content in animals and humans and that in dogs (and therefore most probably in humans also) the isotopic antral cyclical changes paralleled the antral spike activity, i.e., the antral contraction. Not only did we confirm that the mean frequency of gastric contractions in healthy volunteers is ~3/min but also we showed that the amplitude of the contractions decreased in the course of gastric emptying of a physiological test meal. The contraction frequency increase we observed in this study is not consistent with the antral quiescence observed by Rees et al. (17). However, the narrow range of variation we obtained may not be physiologically significant, and in addition, we may have missed a reduction during late emptying by imaging for only 120 min. In contrast, the decrease in amplitude of the antral contractions is in perfect agreement with the observation of Rees et al. that the motor motility index of the distal antrum decreased during the postprandial period. We did not meas-

ure the intragastric consistency of the meal with time and we did not perform animal correlations between the amplitude of the scintigraphic time-activity curves and the antral wall movements with strain gauges. Nevertheless, we believe that the larger amplitudes observed during the early emptying reflects, as in the Rees et al. experiment, the greater excitability of antral phasic contractility by particulate food compared with homogenate foodstuff when digestion proceeds. The absence of variation of the composite time-activity curve parameters PCR, TPCR, PFR, and TPFR suggests that both systolic and diastolic functions of the stomach remain constant throughout the gastric-emptying process in healthy subjects.

Visualization of cardiac contraction and phase analysis of blood-pool scintigrams have been performed in nuclear cardiology for some years using the gating technique (3, 16). In this technique, the cardiac cycle, defined by the electrocardiographic R wave, is divided into multiple intervals to create a composite image made up of multiple frames. Repeatedly viewing these frames in rapid sequence gives the illusion of a beating heart. The lack of a good noninvasive electrical signal to separate gastric cycles hampered the application of this technique to gastric contractions. Therefore, we developed a curve-peak finding algorithm to indicate the start of each gastric cycle, which is then divided into multiple intervals and frames. As in cardiology, the main interest of the closed-loop cinematic display resides in the evaluation of the entire gastric wall motion, which cannot be obtained on a routine basis by other techniques and particularly not by contrast X-rays due to excessive radiation exposure.

By applying this technique to the stomach we were able to confirm that the gastric fundus does not show phasic contractions, whereas in the distal stomach, contractions originate in the midcorpus and propagate aborally to the pylorus.

In conclusion, the scintigraphic test can be used to noninvasively and quantitatively characterize the gastric contractions, thereby allowing a correlation between gastric motor activity and gastric emptying. Better characterization of the pathophysiology of gastric emptying in patients should be enhanced by this technique.

Address for reprint requests: J.-L. C. Urbain, Nuclear Medicine Dept., U. Z. Gasthuisberg, Herestroat 49, 3000 Leuven, Belgium.

Received 2 March 1990; accepted in final form 2 August 1990.

REFERENCES

1. ABELL, T. L., AND J. R. MALAGELADA. Glucagon-evoked gastric dysrhythmias in humans shown by an improved electrogastrographic technique. *Gastroenterology* 88: 1932–1940, 1985.
2. ABELL, T. L., AND J. R. MALAGELADA. Electrogastrography. Current assessment and future perspectives. *Dig. Dis. Sci.* 33: 982–992, 1988.
3. BOTVINICK, E. H., M. W. DAE, J. W. O'CONNELL, M. M. SCHEINMAN, R. S. HATTNER, AND D. B. FAULKNER. First harmonic Fourier (phase) analysis of blood pool scintigrams for the analysis of cardiac contraction and conduction. In: *Cardiac Nuclear Medicine*, edited by M. C. Gerson. New York: McGraw-Hill, 1987, p. 109–148.
5. CANNON, W. B. The movements of the stomach studied by means of the Röentgen rays. *Am. J. Physiol.* 1: 359–382, 1898.
6. CARLSON, H. C., C. F. CODE, AND R. A. NELSON. Motor action of the canine gastroduodenal junction: a cineradiographic, pressure and electric study. *Am. J. Dig. Dis.* 11: 155–176, 1966.
7. EL-SHARKAWY, T. Y., K. G. MORGAN, AND J. H. SZURSZEWSKI. Intracellular electrical activity of canine and human gastric smooth muscle. *J. Physiol. Lond.* 229: 291–307, 1978.
8. EL-SHARKAWY, T. Y., AND J. H. SZURSZEWSKI. Modulation of canine antral circular smooth muscle by acetylcholine, noradrenaline and pentagastrin. *J. Physiol. Lond.* 179: 309–320, 1978.
9. GRIFFITH, G. H., G. M. OWEN, S. KIRKMAN, AND R. SHIELDS. Measurement of the rate of gastric emptying using chromium-51. *Lancet* 1: 1244–1245, 1966.
10. ITOH, Z., I. AIZAWA, R. HONDA, S. TAKEUCHI, AND K. MORI. Regular and irregular cycles of interdigestive contractions in the stomach. *Am. J. Physiol.* 238 (*Gastrointest. Liver Physiol.* 1): G85–G90, 1980.
11. ITOH, Z., S. TAKEUCHI, A. AIZAWA, AND R. TAKAYANAGI. Characteristic motor activity of the gastrointestinal tract in fasted conscious dog measured by implanted force transducers. *Am. J. Dig. Dis.* 23: 229–238, 1978.
12. KING, P. M., R. D. ADAM, A. PRYDE, W. N. MCDICKEN, AND R. C. HEADING. Measurement of gastric emptying by real-time ultrasound. *Gut* 23: 524–527, 1982.
13. KING, P. M., R. D. ADAM, A. PRYDE, W. N. MCDICKEN, AND R. C. HEADING. Relationships of human antroduodenal motility and transpyloric fluid movement: noninvasive observations with real-time ultrasound. *Gut* 25: 1384–1391, 1984.
14. LIND, J. F., H. I. DUTHIE, J. F. SCHEGEL, AND C. F. CODE. Motility of the gastric fundus. *Am. J. Physiol.* 201: 197–202, 1961.
15. MORGAN, K. G., T. C. MUIR, AND J. H. SZURSZEWSKI. The electrical basis for contraction and relaxation in canine fundal smooth muscle. *J. Physiol. Lond.* 311: 475–488, 1981.
16. PARKER, D. A., J. H. THARLL, AND J. W. FROELICH. Radionuclide ventriculography: methods. In: *Cardiac Nuclear Medicine*, edited by M. C. Gerson. New York: McGraw-Hill, 1987, p. 67–84.
17. REES, W. D. W., V. L. W. GO, AND J. R. MALAGELADA. Antroduodenal response to solid liquid and homogenized meals. *Gastroenterology* 76: 1438–1442, 1979.
18. SIEGEL, J. A., R. K. WU, L. C. KNIGHT, R. E. ZELAC, H. S. STERN, AND L. S. MALMUD. Radiation dose estimates for oral agents used in upper gastrointestinal disease. *J. Nucl. Med.* 24: 835–837, 1983.
19. SZURSZEWSKI, J. H. Electrical basis for gastrointestinal motility. In: *Physiology of the Gastrointestinal Tract* (2nd ed.), edited by L. R. Johnson. New York: Raven, 1987, p. 383–422.
20. VANTRAPPEN, G., J. JANSSENS, J. HELLEMANS, AND V. GHOOTS. The interdigestive motor complex of normal subjects and patients with bacterial overgrowth of the small intestine. *J. Clin. Invest.* 59: 1158–1166, 1977.
21. YOU, C. H., K. Y. LEE, W. Y. CHEY, AND R. MENGUY. Electrogastrographic study of patients with unexplained nausea, bloating and vomiting. *Gastroenterology* 79: 311–314, 1980.